A new form of Anhidrotic Ectodermal Dysplasia with Immunodeficiency caused by abolished Store-Operated Ca2+ Entry

Ćuk Mario[1], **Lian** Jayson[2], **Kahlfuss** Sascha[2], **Kozhaya** Lina[3], **Vaeth** Martin[2], **Rieux-Laucat** Frederic[4], **Picard** Capucine[5], **Benson** J. Melina[2], **Jakovčević** Antonia[a], **Bilić** Karmen[a], **Martinac** Iva[b], **Stathopulos** Peter[6], **Kacskovics** Imre[7], **Vraetz** Thomas[8], **Speckmann** Carsten[8c], **Ehl** Stephan[8c], **Issekutz** Thomas[9], **Unutmaz** Derya[3], **Feske** Stefan[2]

[1]Department of Pediatrics, [a]Zagreb University Hospital Centre and [b]School of Medicine, Zagreb, Croatia; [2]Department of Pathology, New York University School of Medicine, New York, NY, USA; [3]The Jackson Laboratory for Genomic Medicine, Framington, USA; [4]INSERM UMR Laboratory of the Immunogenetics of Pediatric Autoimune Diseases, Paris, France and INSERM UMR Imagine Institute, Paris Descartes-Sorbonne, Paris Cite University, Paris, France; [5]INSERM UMR Imagine Institute, Paris Descartes-Sorbonne, Paris Cite University, Paris, France and The Study Center for Primary Immunodeficiencies, Necker-Enfants Malades Hospital, Necker Medical School, Paris, France; [6]Schulich School of Medicine and Dentistry, Western University London, London, United Kingdom; [7]ImmunoGenes, Budapest, Hungary; [8]Center for Pediatrics, University of Freiburg, Freiburg, Germany; [8c]Center for Chronic Immunodeficiency, Medical Centre, University of Freiburg, Freiburg, Germany; [9]Dalhousie University, Halifax, New Scotia, Canada.

BACKGROUND: Calcium signaling is fundamental to many cellular processes. An important pathway for increasing intracellular Ca2+ levels is store-operated Ca2+ entry (SOCE) regulated by stromal interaction molecule (STIM1-2), and Ca2+ channels formed by ORAI1-3 proteins. Mutations in the ORAI1 and STIM1 genes that abolish SOCE cause a combined immunodeficiency (CID) syndrome that is accompanied by autoimmunity and nonimmunologic symptoms.

CASE REPORT: Here we present patients with Anhidrotic Ectodermal Dysplasia with Immunodeficiency (EDA-ID) caused by novel homozygous p.V181SfsX8, p.L194P, and p.G98R mutations in the ORAI1 gene (Fig.1) that suppressed ORAI1 protein expression and SOCE in the patients' lymphocytes and fibroblasts (Figs. 2&3). A unifying feature of patients with null mutations in ORAI1 is EDA. Anhidrosis was present in patients P1 to P4 and confirmed by pilocarpin iontophoresis. Patients had dry and exfoliate skin, and they showed signs of heat intolerance and thermoregulatory instability characterized by several attacks of facial flushing accompanied by tachycardia, tachypnea, and hypertension. A skin biopsy specimen showed the presence of eccrine sweat glands in the dermis demonstrating that anhidrosis is not due to a defect in sweat gland development. Recently, we reported that sweat glands require SOCE for opening of the Ca2+-activated chloride channel TMEM16A and thus chloride secretion and sweat production, pointing that anhidrosis in ORAI1-deficient patients could be functional (Fig.4). ORAI1-deficient patients had severe enamel defects diagnosed as hypocalcified amelogenesis imperfecta type III (Fig.5). In contrast, patients with EDA-ID caused by NF-kB signaling defects also have a tooth defect, which is characterized by hypodontia and conical teeth and thus is morphologically easily distinguishable from the enamel defects in ORAI1-deficient patients. ORAI1-deficient patients showed thin and brittle hair.

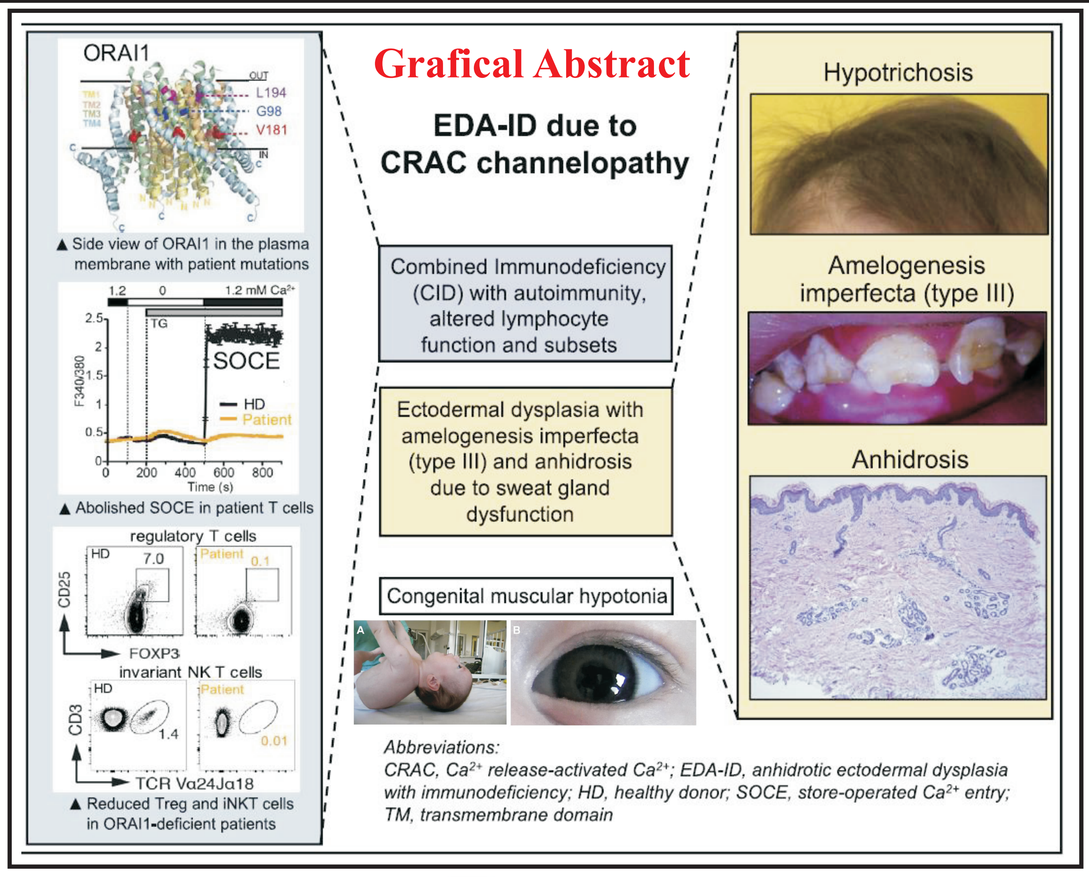

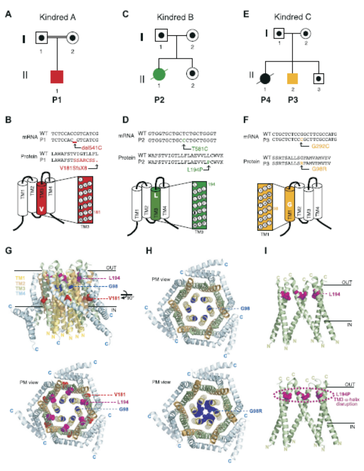

Figure 1.
Three novel ORAI1 mutations.
A-F, Pedigrees (Fig 1, A, C and E) and mRNA/protein sequences of ORAI1 mutations (Fig 1, B, D and F) identified in 3 unrelated kindreds. Fig 1, A and B, Patient P1 (A-II-1) of kindred A is homozygous for a single nucleotide deletion (c.del541C) in exon 2 of ORAI1 that results in a frameshift and premature stop codon in TM3 of ORAI1 protein (p.V181SfsX8). Fig 1, C and D, Patient P2 (B-II-1) is homozygous for a single nucleotide transition (c.T581C) in exon 2 of ORAI1 that results in a single amino acid substitution in TM3 (p.L194P). Fig 1, E and F, Patient P3 (C-II-2) and his sister, patient P4 (C-II-1), are homozygous for a single nucleotide transversion (c.G292C) in exon 1 of ORAI1 that results in a single amino acid substitution in TM1 (p.G98R). In Fig 1, A, C and E, solid symbols represent patients, dots in open symbols represent confirmed heterozygous carriers, and double lines indicate consanguinity. G, Homology model of the hexameric human ORAI1 protein structure modeled on the Drosophila melanogaster Orai crystal structure. Tertiary structure of the ORAI1 hexamer from the side (top) and extracellular side of the plasma membrane (PM) revealing the channel pore (bottom). The inner (IN) and outer (OUT) leaflets of the PM are indicated; TM domains are color coded (TM1, yellow; TM2, orange; TM3, green; and TM4, blue). Amino acid residues mutated in patients P1 to P4 are shown in color (V181, red; L194, magenta; and G98, blue). H and I, Structure models of wild-type (top) and mutant (bottom) ORAI1 (Fig 1, H, p.G98R; Fig 1, I, p.L194P). Models orient the mutant side chains in positions homologous to the wild-type residues and do not show an experimentally determined structure of mutant proteins.

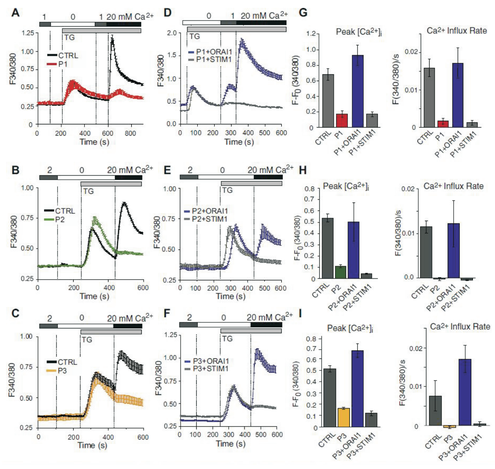

Figure 2.
ORAI1 mutations abolish SOCE.
A-C, SOCE measurements in fibroblasts of patients P1, P2, and P3 and an HD control subject (CTRL). Cells were loaded with Fura-2 and stimulated with thapsigargin (TG) in the absence of extracellular Ca2+, followed by readdition of 20 mmol/L (mM) Ca2+. Traces show intracellular Ca2+ levels (F340/380) recorded by using time-lapse microscopy and represent the average ±SEM of more than 64 cells from 1 representative experiment. D-F, Fibroblasts from patients P1, P2, and P3 were retrovirally transduced with bicistronic vectors encoding wild-type ORAI1 (internal ribosome entry site [IRES]–green fluorescent protein [GFP]) or STIM1 (IRES-GFP). Intracellular Ca2+ levels in GFP1 fibroblasts were measured, as described in Fig 2, A-C. Shown are Ca2+ traces from 1 representative experiment; more than 30 cells were analyzed. G-I, Bar graphs show means ±SEMs of peak intracellular Ca2+ levels after TG stimulation and readdition of 20 mmol/L Ca2+ (left) and the Ca2+ influx rate in the first 20 seconds after readdition of Ca2+ (right). Ca2+ traces in Fig 2, A-F, and bar graphs in Fig 2, G-I, are representative of 2 (patients P2 and P3) and 3 (patient P1) independent experiments.

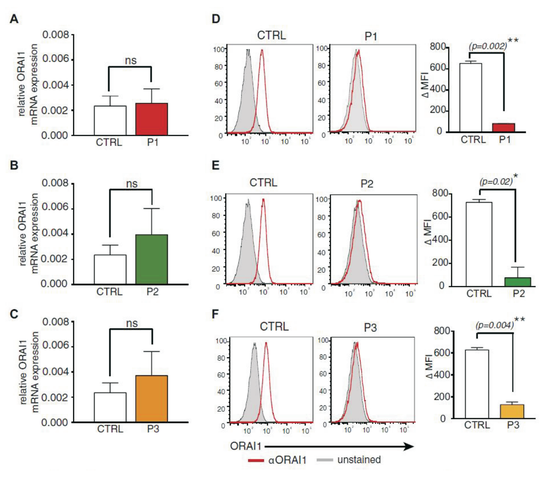

Figure 3.
ORAI1 mutations abolish protein expression.
*A-C, Bar graphs show means ±SEMs of ORAI1 mRNA isolated from fibroblasts of patients P1 (Fig 2, A), P2 (Fig 2, B), and P3 (Fig 2, C) compared with HD control fibroblasts (CTRL) and measured by using quantitative real-time PCR. D-F, Flow cytometric analysis of ORAI1 (red) at the surfaces of fibroblasts from patients P1 (Fig 3, D), P2 (Fig 3, E), and P3 (Fig 3, F) and HD control fibroblasts (CTRL) using an antibody against the second extracellular domain of ORAI1. Unstained fibroblasts were used as controls (gray). Bar graphs show the average of Δ mean fluorescence intensities (ΔMFIs; calculated as MFIORAI1 - MFIunstained control) ±SEM. Data in Fig 3, A-C and D-F, represent 2 independent experiments for each patient. Statistical significance was calculated by using the unpaired Student t test: *P < .05 and **P < .01.*

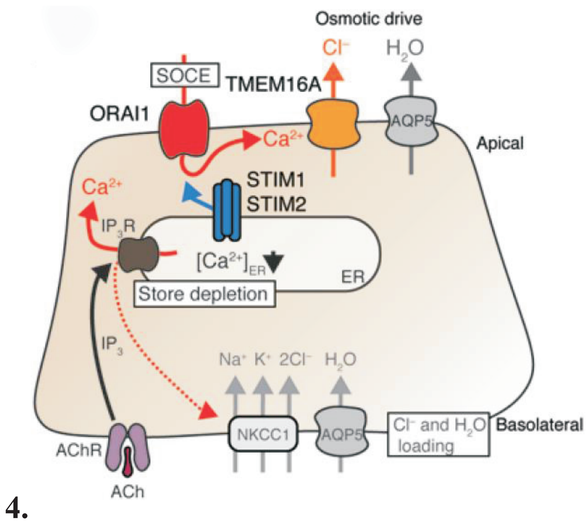

Figure 4.
SOCE-induced TMEM16A activation and Cl⁻ secretion.
AChR stimulation results in IP3-mediated release of Ca2+ from ER stores, which activates STIM1 and STIM2, allowing them to bind to and open the store-operated CRAC channel ORAI1. SOCE via ORAI1 activates TMEM16A Cl⁻channels and Cl⁻secretion, which provides the osmotic driving force for water flow and sweat production (Ref: 5).

Figure 5.
Hypocalcified amelogenesis imperfecta.
Photograph of the teeth of a patient with ORAI1 p.R91W mutation that abolishes SOCE. Shown here is the lower jaw at approximately 6 years of age. All erupted teeth have lost their enamel capping on the occlusal surfaces and only remnants can be seen on the lateral margins of the teeth (arrows). The yellowish appearance of the teeth is related to dentine exposure (Refs: 2&3).

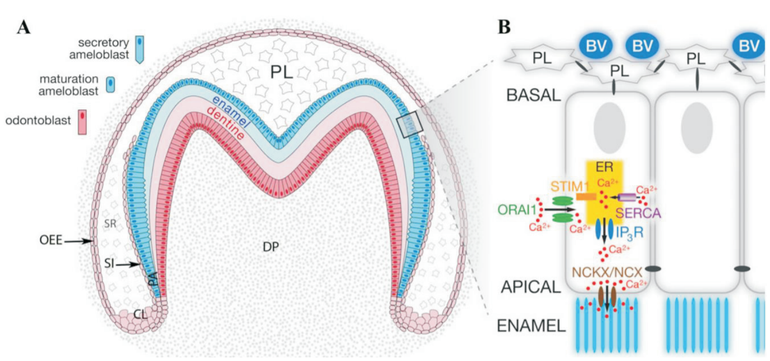

Figure 6.
Tooth, enamel cells and the Ca2+ transport model.
(A) Schematic section of a human molar showing the location of enamel forming cells, ameloblasts, in relation to other structures and cells. The main structures found in a tooth are the outer enamel layer, the dentine (formed by odontoblasts) and the innermost dental pulp. Secretory ameloblasts are epithelium-derived cells arising from pre-ameloblasts (PA) at the cervical loop (CL). The cells undergo morphological changes including increases in height, and develop a specialized secretory process at the distal (apical) end of the cell. Secretory ameloblasts reorganize into maturation stage ameloblasts once the thickness (volume) of enamel tissue has been completed. Maturation stage ameloblasts are shorter, loose the secretory process (Tomes' process) and switch their functional properties to become cells specialized in transport. (B) Representative model of maturation stage ameloblasts showing the localization of ORAI1 and STIM1 in the plasma membrane and ER, respectively. This working model of Ca2+ transport in ameloblasts builds on the model proposed by Hubbard. It postulates that Ca2+ enters through PM Ca2+ channels and is taken up into the ER at the basolateral pole of the cell, and released into the cytoplasm via IP3R or RyR at the apical pole, where it is secreted into the extracellular enamel matrix. The emerging details and molecular components of this Ca2+ transport need to be investigated further, but our recent data suggest that STIM1 and ORAI1 mediate Ca2+ uptake whereas NCKX/NCX exchangers mediate Ca2+ extrusion. Abbreviations: BV, blood vessels; DP (dental pulp); NCKX, Na+/Ca2+-K+ exchanger; NCX, Na+/Ca2+ exchanger; OEE (outer enamel epithelium); PL (papillary layer); SERCA, Sarco/endoplasmic reticulum Ca2+ ATPase; SI (stratum intermedium); SR (stellate reticulum) (Ref 4).

RESULTS: Patients had dry/exfoliate skin, thin/brittle hair, heat intolerance/thermoregulatory instability, attacks of facial flushing, tachycardia, tachypnea, hypertension, anhidrosis, impared eccrine sweat glands due to Ca2+-activated chloride channel TMEM16A dysfunction, severe enamel defects. Conventional T/B cells development and numbers were preserved compared to their function. T cells showed reduced/absent proliferation in response to PHA, decreased IL-2, IL-22, TNF-α, and IFN-γ production contributing to ID. Patients had lymphadenopathy/hepatosplenomegaly, autoantibodies-mediated pancytopenia, antiphospholipid syndrome, loss of naive CD45RA+ T cells and concomitant expansion of CD45RO+ or HLA-DR+ activated T cells, decreased percentages of CD25+FOXP3+ Treg cells and CD25+CD127+ T cells, reduction of Treg cells in CD45RA+FOXP3+ naive and CD45RA+FOXP3+ activated Treg cells suggesting that SOCE is required for maintaining immunological tolerance. Patients had generalized CM, iris hypoplasia and mydriasis caused by mitochondrial disfunction as we recently reported (grafical abstract).

DISCUSSION: To date, the diagnosis of EDA-ID is limited to patients with defects in NF-kB signaling who are prone to infections with mycobacteria, P.jirovecii, Candida albicans, and, most frequently, pyogenic bacteria caused by hypogammaglobulinemia and failure to mount a specific antibody response to polysaccharide antigens. In contrast, ORAI1-deficient patients are susceptible to an overlapping spectrum of pathogens, but they are also prone to viral infections, including CMV, EBV, RSV, and rotavirus. In addition, AIHA and autoimmune thrombocytopenia are also common in SOCE deficient patients but not NF-kB; instead, patients with NF-kB defects can have inflammatory bowel disease (NF-kB essential modulator colitis). Also, ORAI1 mutations were associated with impaired T cell function and reduced numbers of invariant iNKT cells and regulatory FOXP3+ Treg cells, and altered composition of γδT cell and natural killer cell subsets

CONCLUSION: We propose that mutations in ORAI1 that abolish SOCE constitute a new form of EDA-ID and are an important differential diagnosis of EDA-ID caused by defects in NF-kB signaling.

***References:* 1.** *Lian J*, Ćuk M* and Kahlfuss S* et al. ORAI1 mutations abolishing store-operated Ca2 entry cause anhidrotic ectodermal dysplasia with immunodeficiency. J Allergy Clin Immunol. 2017 Nov 16. pii: S0091-6749(17)31763-3. doi: 10.1016/j.jaci.2017.10.031. [Epub ahead of print]. *These authors contributed equally to this work.* ***Abstract presenting and corresponding author: Mario Ćuk,* MCuk@kbc-zagreb.hr*; Lead Corresponding author: Stefan Feske,* stefan.feske@nyumc.org*; 2.** *Feske S et al. A mutation in Orai1 causes immune deficiency by abrogating CRAC channel function. Nature 2006; 441:179–185.; **3.** McCarl CA et al. ORAI1 deficiency and lack of store-operated Ca2+ entry cause immunodeficiency, myopathy, and ectodermal dysplasia. The Journal of allergy and clinical immunology 2009;124:1311–1318 e1317.; **4.** Lacruz RS & Feske S. Diseases caused by mutations in ORAI1 and STIM1. Ann N Y Acad Sci, 2015;1356:45-79.; **5.** Concepcion AR et al. Store-operated Ca2+ entry regulates Ca2+-activated chloride channels and eccrine sweat gland function. J Clin Invest. 2016;126:4303-4318.*